

## Damage process of high purity tungsten coatings by hydrogen beam heat loads

S. Tamura<sup>a,\*</sup>, K. Tokunaga<sup>b</sup>, N. Yoshida<sup>b</sup>, M. Taniguchi<sup>c</sup>, K. Ezato<sup>c</sup>,  
K. Sato<sup>c</sup>, S. Suzuki<sup>c</sup>, M. Akiba<sup>c</sup>, Y. Tsunekawa<sup>a</sup>, M. Okumiya<sup>a</sup>

<sup>a</sup> Toyota Technological Institute, 2-1-2 Hisakata, Tempaku, Nagoya 468-8511, Japan

<sup>b</sup> Research Institute for Applied Mechanics, Kyushu University, Kasuga, Fukuoka 816-8580, Japan

<sup>c</sup> Naka Fusion Research Establishment, Japan Atomic Energy Research Institute, Ibaraki 311-01, Japan

### Abstract

To investigate the synergistic effects of heat load and hydrogen irradiation, cyclic heat load tests with a hydrogen beam and a comparable electron beam were performed for high purity CVD-tungsten coatings. Surface modification was examined as a function of the peak temperature by changing the heat flux. Scanning Electron Microscopy analysis showed that the surface damage caused by the hydrogen beam was more severe than that by the electron beam. In the hydrogen beam case, cracking at the surface occurred at all peak temperatures examined from 300 °C to 1600 °C. These results indicate that the injected hydrogen induces embrittlement for the CVD-tungsten coating.

© 2004 Elsevier B.V. All rights reserved.

PACS: 81.40.N; 41.75.A

Keywords: Tungsten; Hydrogen; Ion irradiation; Electron beam heating; Defects

### 1. Introduction

The ductile to brittle transition temperature (DBTT) of tungsten is about 400 °C, and this DBTT is raised by the grain growth after annealing above the recrystallization temperature (about 1300 °C). It was reported that tungsten materials showed the best heat load performance in the temperature range between the DBTT and the recrystallization temperature [1].

The armor of the high heat flux components in fusion reactors will suffer from not only heat loads but also from very high particle fluxes, such as the hydrogen fuel.

It is easy to imagine that the hydrogen injected in the material may affect some properties of the materials and change the heat load performance, because the flux of hydrogen is very high and it can penetrate deep by thermal migration. In fact, it was reported that the severe embrittlement of tungsten specimens was observed after exposure to hydrogen plasmas of long duration discharges in TRIAM-1M [2]. This result indicates that the mechanism of synergistic damage to tungsten by hydrogen irradiation and heat loading should be investigated.

From the view point of synergistic damage process under simultaneous heat loading and hydrogen bombardment, cyclic heat load tests have been performed with both hydrogen and electron beams on CVD-tungsten coated W–30Cu composites.

\* Corresponding author. Tel.: +81 052 809 1857; fax: +81 052 809 1857.

E-mail address: [tamura@toyota-ti.ac.jp](mailto:tamura@toyota-ti.ac.jp) (S. Tamura).

## 2. Experimental

### 2.1. Specimen

High purity (99.99998%) tungsten coating on tungsten infiltrated copper (W-30Cu) blocks was manufactured by Tokyo Tungsten Co. Ltd. using chemical vapor deposition (CVD) techniques. The thickness of the coating was 5 mm and the size of the specimens was 30 mm × 30 mm × 30 mm. The coefficient of thermal expansion of the tungsten infiltrated copper is 70% less compared to pure copper [3]. No cracks and defects were found on the surface of the samples before the heat load tests.

### 2.2. Experimental equipment and loading conditions

Cyclic heat load tests with a hydrogen beam were performed at the Particle Beam Engineering Facility (PBEF) [4] in JAERI, while those with an electron beam were performed at the JAERI Electron Beam Irradiation Stand (JEBIS) [5]. The test sample was mechanically fixed by a screw on a copper heat sink, which was actively cooled with flowing water. The design of the heat sink for the two heat load facilities is identical.

The experimental conditions of the cyclic heat load tests are listed in Table 1. Power and duration of the beam were adjusted to obtain peak surface temperatures below DBTT, between the DBTT and the recrystallization temperature, and above the recrystallization temperature. The local surface temperature distribution of the specimen under the cyclic heat loading was measured with an IR camera. Each sample was equipped with a thermocouple embedded in a groove located on the side of the substrate, as shown in Fig. 1. The tip of the thermocouple is placed at the joint interface between the coating and the substrate. Profiles of heat fluxes were measured with a calorimeter. Changes of the surface morphology were observed by Scanning Electron Microscopy (SEM).

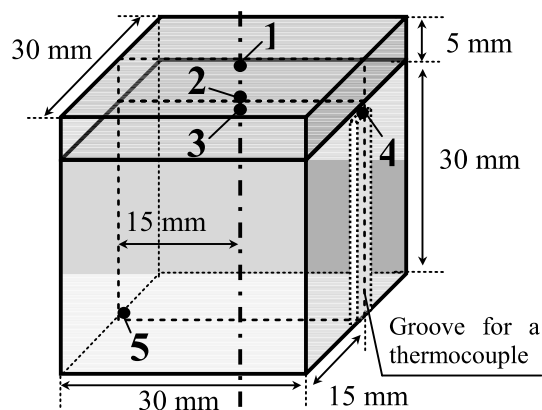


Fig. 1. Sample geometry and dimensions.

## 3. Results

### 3.1. Below the DBTT (about 300 °C)

Fig. 2 shows the SEM-images of the coating surfaces exposed to the cyclic heat loads with the hydrogen beam and the electron beam. After 100 shots, no visible surface modification was observed on the surfaces of both samples. After 250 shots, a large crack with a length of about 4 mm was formed at the center of the coating for the hydrogen beam exposure, but only fine cracks of about 50 μm in length were seen for the electron beam loading.

### 3.2. Between DBTT and recrystallization temperature (about 650 °C)

Fig. 3 shows the change of the surface morphology of the coating after the cyclic heat load tests. After 150 shots, no visible surface modification was detected on the surfaces of either sample. After 300 shots, however, a crack with a length of about 180 μm was observed at the center of the coating surface loaded by the hydrogen beam. On the contrary, any defects such as cracks were

Table 1

The experimental conditions of the cyclic heat loading

	Base temperature [°C]	Peak surface temperature [°C]	Peak temperature at the joint interface of the side part of the substrate [°C]	Absorbed heat flux of H <sup>+</sup> -beam or e-beam [MW/m <sup>2</sup> ]	Beam duration [s]	Flux of hydrogen [H/m <sup>2</sup> s]	Acceleration voltage of hydrogen beam [kV]
≤DBTT	R.T.	298 ± 7	97 ± 4	4.9 ± 0.2	1.0	1.9 × 10 <sup>21</sup>	18
Between DBTT and recrystallization temperature	R.T.	653 ± 16	204 ± 11	9.8 ± 0.3	1.0	2.5 × 10 <sup>21</sup>	24
>Recrystallization temperature	122 ± 4	1602 ± 27	682 ± 14	15.2 ± 0.5	3.0	4.0 × 10 <sup>21</sup>	24

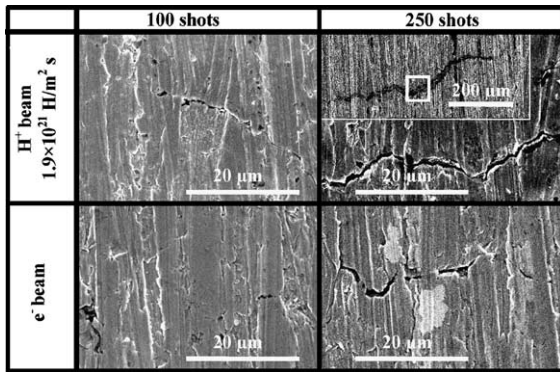


Fig. 2. Surface morphology of the samples after cyclic heat loading with a peak temperature of 300 °C.

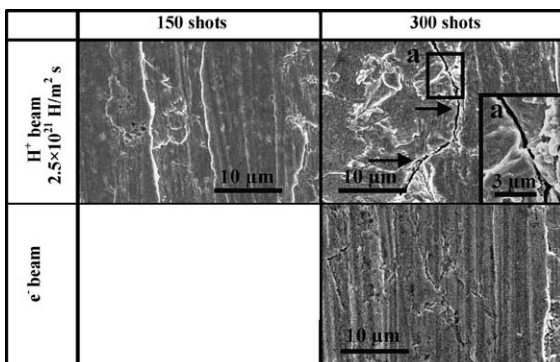


Fig. 3. Surface morphology of the samples after cyclic heat loading with a peak temperature of 650 °C.

not observed for the sample loaded by the electron beam.

### 3.3. Above the recrystallization temperature (about 1600 °C)

After a cyclic heat load of 110 shots, cracks with a width of about 5 μm and with a length of over 10 mm were observed on both samples. Typical cracks are shown in Fig. 4. No clear differences in the crack size between the two samples were seen, but small pores with a diameter of < 0.2 μm as shown in Fig. 4(b) were observed around the edges of cracks on the hydrogen-irradiated surface.

Judging from the cooling down rate of the surface temperature, which can be detected as the change of color, the cracking along the joint interface at a corner of the coating edge was caused by 64 shots of hydrogen beam exposure with  $15 \text{ MW/m}^2 \times 3 \text{ s}$ . In spite of the separation at a corner of the coating edge, the peak temperature at the coating surface remained about 1600 °C during a subsequent shot. However the cooling rate of

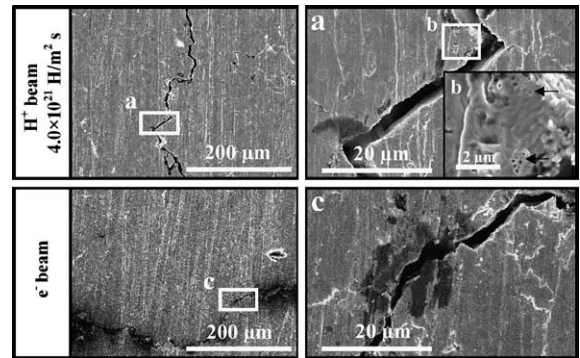


Fig. 4. Surface morphology of the samples after 110 shots with a peak temperature of 1600 °C. Small pores are observed at the coating surface (b) after hydrogen beam irradiation.

the coating surface at the end of a subsequent shot was decreased. This result means that the heat transfer at the joint interface is relatively poor.

## 4. Discussions

### 4.1. Time evolution of temperature distribution during a heat load of $15 \text{ MW/m}^2$

To estimate the hydrogen diffusion behavior, the temperature distribution in a sample is required. Three-dimensional temperature distributions in the samples were calculated using the finite-difference method (FDM). To obtain the best fit to the experimental result of the first shot, the following parameters were derived from the fitting procedure: the heat transfer coefficient at the joint interface of the coating is 9.5% of the theoretical value, the heat transfer coefficient at the bottom interface of the sample is estimated to be  $6000 \text{ W/m}^2 \text{ K}$ , and the emissivities of the coating and the substrate are 0.22 and 0.50, respectively. Fig. 5 shows the calculated time evolution of the temperature distribution in the sample heated with a heat flux of  $15 \text{ MW/m}^2$  for 3 s duration. This result indicates that the calculation using the above conditions can simulate the experimental results, i.e., the fixed conditions stated above are appropriate to this experimental system.

### 4.2. Accumulation of implanted hydrogen for $4.0 \times 10^{21} \text{ H/m}^2 \text{ s}$ ( $15 \text{ MW/m}^2$ ) exposure

To investigate the hydrogen diffusion behavior in the hydrogen-beam-heated sample, the time evolution of hydrogen distribution in the sample was estimated by numerical calculation using FDM. Taking into account Fick's law and the Soret-effect [6], the solute flux  $J$  in the matrix can be written as

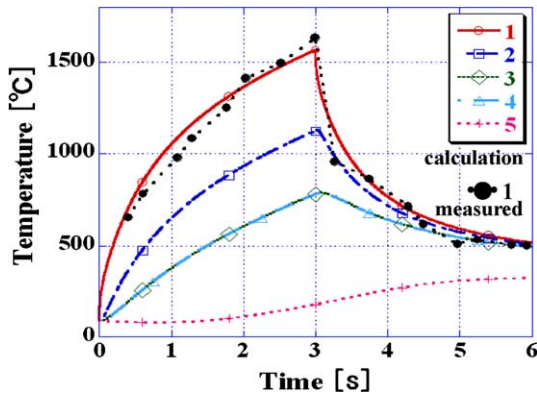


Fig. 5. Calculated time evolution of the temperature distribution in a sample heated with a heat flux of 15 MW/m<sup>2</sup> for 3 s. Numbers 1–5 in the graphs represent point numbers (see Fig. 1). Point number 4 indicates the position of the thermocouple.

$$J = -D \left( \nabla C + C \frac{Q^*}{RT^2} \nabla T \right), \quad (1)$$

where  $T$  [K] is the temperature,  $D = D(T)$  is the diffusion coefficient,  $C$  the concentration of the solute,  $Q^*$  the heat of transport, and  $R$  is the gas constant. The re-emission flux  $\Phi$  of hydrogen molecules at the sample surface [7,8] is expressed as

$$\Phi = K_r C^2 \quad [\text{H}_2/\text{cm}^2 \text{ s}], \quad (2)$$

where  $K_r$  is the recombination coefficient of hydrogen atoms. The calculation of the hydrogen distribution is carried out based on these relations. The diffusion coefficient  $D(T)$  of hydrogen in tungsten is given by [9]

$$D(T) = 4.1 \times 10^{-3} \exp(-3.9 \times 10^4 [\text{J/mol}]/RT) \quad [\text{cm}^2/\text{s}]. \quad (3)$$

Also, the recombination coefficient  $K_r(T)$  of hydrogen atoms at the tungsten surface is given by [10]

$$K_r(T) = 3.2 \times 10^{-23} \exp(-1.15 \times 10^5 [\text{J/mol}]/RT) \quad [\text{cm}^4/\text{s}]. \quad (4)$$

The coefficients  $D(T)$  and  $(K_r)(T)$  for copper are [7]:

$$D(T) = 3.0 \times 10^{-4} \exp(-1.34 \times 10^5 [\text{J/mol}]/RT) \quad [\text{cm}^2/\text{s}], \quad (5)$$

$$K_r(T) = 1.0 \times 10^{-24} \exp(-1.04 \times 10^5 [\text{J/mol}]/RT) \quad [\text{cm}^4/\text{s}]. \quad (6)$$

The heats of transport  $Q^*$  of tungsten and copper were given the tentative values  $-2.0 \times 10^{-4}$  J/mol and  $-4.0 \times 10^{-3}$  J/mol, respectively [11]. Using the above diffusion and the recombination coefficients, the time evolution of the temperature distribution in a sample is calculated with the conditions discussed in Section 4.1. The actual transmission area of the solute hydrogen at the joint interface of the coating is estimated from the result of Section 4.1 to be 9.5% of the whole area at the joint interface. From the hydrogen distribution width calculated using the TRIM-code, the thickness of the elements at the coating surface was adopted at 0.2  $\mu\text{m}$ .

Fig. 6 shows the calculated time evolution of the hydrogen distribution along the center axis of the sample irradiated with a hydrogen beam of 15 MW/m<sup>2</sup> ( $4.0 \times 10^{21}$  H/m<sup>2</sup> s) for 3 s. Judging from the result of the calculated time evolution of the hydrogen distribution, hydrogen is hardly released from the sample after a shot. The high cooling rate of the sample appears to be causing this effect. These results indicate that the hydrogen concentration in the sample is increased with increasing number of hydrogen beam shots, and it also indicates that the hydrogen accumulation at the joint interface of the coating causes degradation in its adhesion property.

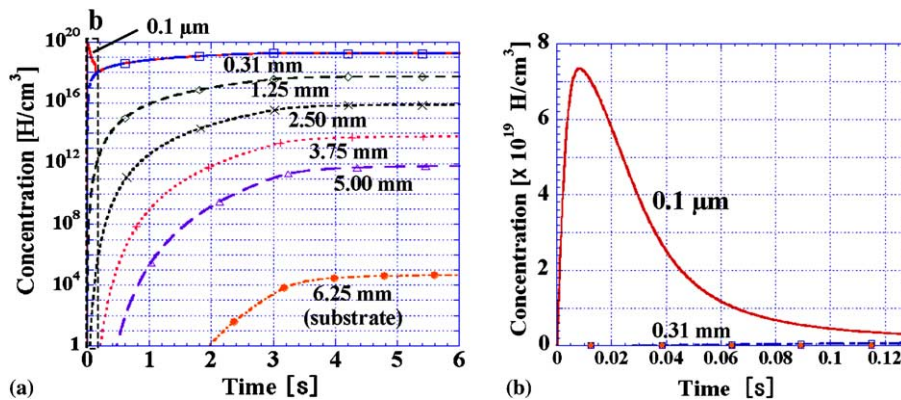


Fig. 6. Calculated time evolution of the hydrogen distribution along the center axis of the sample. Distances indicated in the graphs represent the positions of the center of each FDM element from the coating surface.

### 4.3. Embrittlement of the coating

Under the loading condition with the peak temperature in the range between the DBTT and the recrystallization temperature, the CVD-tungsten coating which was loaded by a cyclic pulse electron beam, shows good thermal shock resisting properties. In spite of this good thermal resisting condition for tungsten, cracks with a length of about 180  $\mu\text{m}$  were observed on the coating surface after the cyclic heat load of a hydrogen beam.

In the cyclic heat load tests with the peak temperature below the DBTT, the cracks formed on the CVD-tungsten coating surface by a cyclic heat load of a hydrogen beam are larger than that of the sample which was loaded by a cyclic electron beam. These cracks on the coating surface are formed by the tensile stress at the coating surface during the cooling stage after each shot [1]. These results indicate that the tungsten coating becomes more brittle by the hydrogen beam irradiation during cyclic heat loading. Also, it means that the rising of the DBTT of the coating surface was caused during cyclic heat loading.

After the cyclic heat load experiment with a peak temperature of about 1600  $^{\circ}\text{C}$ , no clear difference in the crack size was observed for the samples exposed to hydrogen and electron beams. Regarding the change of mechanical properties, such as the embrittlement, this result indicates that the influence of the recrystallization is larger than that of the hydrogen irradiation.

## 5. Conclusions

- (1) In the cyclic heat load experiments with the loading conditions corresponding to peak temperatures of about 300  $^{\circ}\text{C}$  (below the DBTT), the tungsten coating is further embrittled by hydrogen beam irradiation during the cyclic heat loading.
- (2) Under loading conditions with peak temperatures of about 650  $^{\circ}\text{C}$  (between the DBTT and the recrystallization temperature), the CVD-tungsten coating shows good thermal shock-resisting properties under electron beam loading. However, under the

same heating condition using hydrogen beams of 10  $\text{MW}/\text{m}^2$  ( $2.5 \times 10^{21}$   $\text{H}/\text{m}^2 \text{ s} \times 1 \text{ s}$ ), an increase of the DBTT of the coating surface during the cyclic heat loading has been observed.

- (3) Under loading conditions with peak surface temperatures at about 1600  $^{\circ}\text{C}$  (above the recrystallization temperature), the exfoliation of the joint interface at a corner of the coating occurs due to fatigue effects caused by the cyclic hydrogen beam. It also indicates that the hydrogen accumulation at the joint interface of the coating causes degradation of its adhesion property.

## Acknowledgment

This work was a collaborative study with the Japan Atomic Energy Research Institute.

## References

- [1] S. Tamura, K. Tokunaga, N. Yoshida, J. Nucl. Mater. 307–311 (2002) 735.
- [2] N. Yoshida, Y. Hirooka, J. Nucl. Mater. 258–263 (1998) 173.
- [3] I. Smid, M. Akiba, G. Vieider, L. Plöchl, J. Nucl. Mater. 258–263 (1998) 160.
- [4] K. Sato, K. Nakamura, S. Suzuki, M. Araki, M. Dairaku, K. Yokoyama, M. Akiba, Fus. Technol. 30 (1996) 769.
- [5] J. Boscary, S. Suzuki, K. Nakamura, T. Suzuki, M. Akiba, Fus. Eng. Des. 39&40 (1998) 537.
- [6] K. Ashibe, K. Ebisawa, J. Nucl. Mater. 128&129 (1984) 739.
- [7] R.A. Anderl, D.F. Holland, G.R. Longhurst, J. Nucl. Mater. 176&177 (1990) 683.
- [8] A.A. Pisarev, S.K. Zhdanov, O.V. Ogorodnikova, J. Nucl. Mater. 211 (1994) 127.
- [9] V.Kh. Alimov, B.M.U. Scherzer, J. Nucl. Mater. 240 (1996) 75.
- [10] R.A. Anderl, D.F. Holland, G.R. Longhurst, R.J. Pawelko, C.L. Trybus, C.H. Sellers, Fus. Technol. 21 (1992) 745.
- [11] Glen. R. Longhurst, J. Nucl. Mater. 131 (1985) 61.